Transactions of the **14th International Conference on Structural Mechanics in Reactor Technology** (SMiRT 14), Lyon, France, August 17-22, 1997 **G04/4**

Elastic plastic fracture analysis of elliptical circumferential surface flaws in cylinders under pressure and bending

Barthelet B.[1], **Valeta M.P.**[2]
(1) EDF, France
(2) CEA, France

ABSTRACT :

This paper presents a study performed by E.D.F. and CEA to develop J integral solutions for elliptical circumferential surface flaws in cylinders under pressure and bending.
An austenitic steel pipe is considered (R/t=5). A large number of 3-D elastic plastic finite element analyses of surface cracked cylinders with various flaw depths (a/t=1/8, 1/4, 1/2) and flaw aspect ratios (a/c=1/10, 1/3, 1) are carried out using 3-D finite element meshes.
The 3-D finite element computations are used to validate a simplified estimation of J-integral based on R6 rule. A general expression of the parameter Lr (measure of proximity of plastic yielding) is proposed under bending and combination of pressure and bending.

1 INTRODUCTION

Inservice inspection of nuclear components sometimes reveals the presence of flaws. In France, a flaw that exceeds the standards of the RSE-M Code [1] needs to be repaired or evaluated by a numerical fracture mechanics study. This study must prove the flaw to be acceptable for continued service during the evaluated time period. J-integral is widely recognized as the key parameter for flaw assessment under the presence of large inelastic deformation. The development of simplified estimations of J integral, which do not require full numerical calculation for cracked structures, appears very useful. Therefore, Electricité de France, Framatome and CEA are promoting simplified evaluations of J in the RSE-M Code flaw assessment procedure.
This paper presents a study performed by E.D.F. and CEA to develop J-integral solutions for elliptical circumferential surface flaws in cylinders under pressure and bending.

2 FINITE ELEMENT MODEL

2.1 *Geometry*

The analyzed pipe has a mean radius of R = 300 mm and a wall thickness of t = 60 mm.
The model length is 8 times the mean radius.

Six elliptical circumferential inner surface flaws are considered corresponding the following geometries (a is the flaw depth, c is the half flaw length) :

a/t = 1/8 a/c = 1/10 a/t =1/4 a/c = 1/10 a/t =1/2 a/c = 1/3
a/c = 1/3 a/c = 1/3 a/c = 1

Three dimension finite element analyses of the cracked cylinders are carried out using 3-D finite element meshes with detailed crack tip modeling all along the crack front.

2.2 *Material*

The pipe is made of austenitic stainless steel. The stress-strain curve is determined by a Ramberg-Osgood law :

$$\frac{\varepsilon}{\left(\frac{S_y}{E}\right)} = \left(\frac{\sigma}{S_y}\right) + \alpha\left(\frac{\sigma}{S_y}\right)^n \quad (1) \text{ with } \alpha = 3,\ n = 5$$

yield strength S_y = 120 MPa, modulus of elasticity E= 177000 MPa, Poisson's ratio ν = 0,3.

2.3 *Loadings*

Two loagings are analyzed. The first is an increasing bending moment. The second consists in internal pressure of 21,2 MPa (applied on the crack lips too, with the corresponding far field axial force) applied prior to an increasing bending moment.

3 CALCULATION OF J-INTEGRAL

The CASTEM 2000 [2] finite element program is used. J-integral is calculated in elastic and elastic plastic analyses by the G-thêta method ([2] virtual crack extension method).

3.1 *Elastic computations*

Elastic J-integral (J_e = G) is computed for the six cracked pipes under a bending moment (M_x=19.04 10^6 N.mm) and a combination of pressure and bending (P=1 MPa + M_x=19.04 10^6 N.mm). The stress intensity factors are computed using the relation $K_I = \sqrt{\frac{GE}{(1-\nu^2)}}$ (2)

For pressure, the axial stress and the stress intensity factor are writen as follows :

$$\sigma = \sigma_0 + \sigma_1\left(\frac{x}{t}\right) + \sigma_2\left(\frac{x}{t}\right)^2 + \ldots \ (3) \Rightarrow K_I = \left[i_0\sigma_0 + i_1\sigma_1\left(\frac{a}{t}\right) + i_2\sigma_2\left(\frac{a}{t}\right)^2 + \ldots\right]\sqrt{\pi a} \quad (4)$$

For bending $\sigma_b = \frac{MR_e}{I}$ (5) $\Rightarrow K_I = F_b\,\sigma_b\,\sqrt{\pi a}$ (6)

The values of i_0 and F_b are given in table 1 and are consistant with previous studies [3], [4].

3.2 *Elastic plastic computations*

Elastic plastic J-integral J_p is computed for the six cracked pipes :

- under a bending moment (6 step-by-step elastic plastic computations)
- under internal pressure of 21,2 MPa followed by a bending moment (6 computations).

Elastic J-integral (J_e = G) and elastic plastic J-integral values J_p are given for the flaw a/t=1/4, a/c=1/3 as function of M_x in table 2 and P+M_x in table 3.

4 SIMPLIFIED METHOD

The 3-D elastic plastic finite element computations are used to validate a simplified estimation of J integral based on R6 rule. The simplified method gives an evaluation of the elastic plastic J-integral J_p as function of the elastic J-integral J_e and a parameter K_r :

$$J_p = \frac{J_e}{K_r^2} \quad (7) \quad \text{with } K_r \text{ determined } K_r = \left[\frac{E\varepsilon}{L_r S_y} + \frac{L_r^3 S_y}{2 E \varepsilon} \right]^{-\frac{1}{2}} \quad (8)$$

For small flaws, the general expression of the parameter Lr (measure of proximity of plastic yielding) is proposed under bending and combination of pressure and bending :

$$L_r = \frac{1}{S_y} \left[\frac{3}{4} \left(\frac{PD}{2t} \right)^2 + \left(\frac{M_x}{0,95 D^2 t q_x} \right)^2 \right] \quad (9)$$

where P is internal pressure, D the mean diameter, t the thickness, M_x the bending moment.

Small elliptical circumferential flaws do not lower pressure limit load.
q_x is the inertia reduction coefficient due to the flaw and is defined by the following formulas :

for an inner surface flaw : $\gamma = \frac{c}{R_i}$ and $a_1 = a\left(1 - \frac{(t-a)}{D}\right)$ $a_2 = a\left(1 - \frac{2(t-a)}{D}\right)$.

for an outer surface flaw : $\gamma = \frac{c}{R_e}$ and $a_1 = a\left(1 + \frac{(t-a)}{D}\right)$ $a_2 = a\left(1 + \frac{2(t-a)}{D}\right)$.

- si $\gamma \le \frac{\frac{\pi}{2}}{\left(1 - \frac{a_1}{2t}\right)}$ $\quad q_x = \cos\left(\frac{\gamma a_1}{2t}\right) - \frac{a_2}{2t} \sin\gamma \quad (10)$

- si $\gamma > \frac{\frac{\pi}{2}}{\left(1 - \frac{a_1}{2t}\right)}$ $\quad q_x = \cos\left(\frac{(\pi - \gamma) a_1}{2t\left(1 - \frac{a_1}{t}\right)} \right)\left(1 - \frac{a_2}{t}\right) + \frac{a_2}{2t} \sin\gamma \quad (11)$

These expressions are valid if $\frac{a}{t} \le \frac{1}{2}$.

4.1 *Bending*

For various flaw geometries in bending, figures 1 to 3 compare K_r values of equations (8) and (9), and corresponding values obtained from finite element elastic plastic computations $\left(J_e / J_p\right)^{1/2}$.

The simplified method gives good results at the deepest point and the surface point. It is a little unconservative only for the deep and short crack (a/t=1/2, a/c=1) because the local effect is stronger in that case.

4.2 *Pressure + bending*

For various flaw geometries under pressure plus bending, figures 4 to 6 compare K_r values of equations (8) and (9), and corresponding values obtained from finite element elastic plastic computations $\left(J_e/J_p\right)^{1/2}$. The simplified method gives also good results at the deepest point and the surface point.

5 CONCLUSION

A large number of elastic plastic three dimensionnal finite element computations have been carried to validate a simplified method for circumferential flawed pipes. The simplified method gives good results at the deepest point and the surface point for various flaws under bending and combination of pressure and bending. It is a little unconservative only for the deep and short crack (a/t=1/2, a/c=1) because the local effect is stronger in that case.

The present results can be readily used with J-resistance curve approach to predict crack initiation, stable crack growth and instability load in flawed piping systems.

The proposed simplified method will be codified in the RSE-M Code with validity limits (a/t<1/2).

6 REFERENCES

[1] RSE-M code 1997 planned edition Rules for inservice inspection of nuclear powerplant components

[2] CASTEM 2000 Finite element program developped by C.E.A./DMT/SEMT/LAMS

[3] X. Suo and A. Combescure, Application of Gtheta method and its comparison with De Lorenzi approach, Nuclear Engineering, No 135, 1992, pp207-224.

[4] M.Bergman, Stress intensity factors for circumferential surface cracks in pipes.Fatigue Fracture Engineering Materials and structures. Vol.18, No.10, 1995,pp1155-1172.

[5] C. Poette and S. Albaladejo, Stress intensity factors and influence functions for circumferential surface cracks in pipes. Engineering fracture Mechanics, Vol. 39, No. 4, 1991, pp 641-650.

Table 1 Geometry factors from elastic J-integral
(a/t=1/4, a/c=1/3)

a/t	a/c	i0 deepest	i0 surface	Fb deepest	Fb surface
0.25	0.1	1.169	0.533	0.989	0.358
0.125	0.33	0.951	0.635	0.796	0.530
0.25	0.33	0.981	0.666	0.837	0.550
0.50	0.33	1.083	0.752	0.945	0.609
0.50	1	0.668	0.788	0.594	0.665
0.125	0.1	1.093	0.504	0.911	0.408

Table 2 Elastic and elastic plastic J-integral (kJ/m^2)
under bending (a/c=1/4, a/c=1/3)

pressure	moment kNm	Je deepest	Jp deepest	Je surface	Jp surface
0.	0.00E+00	0.	0.	0.	0.
0.	5.15E+08	0.185	0.184	0.08	0.081
0.	1.03E+09	0.737	0.856	0.319	0.372
0.	1.41E+09	1.388	2.12	0.601	0.854
0.	1.79E+09	2.237	4.89	0.968	1.82
0.	2.17E+09	3.287	10.9	1.423	3.86
0.	2.55E+09	4.548	23.5	1.969	8.08
0.	2,94E+09	6.035	48.6	2.612	16.5
0.	4.08E+09	11.65	303.	5.043	109.
0.	5.23E+09	19.095	897.	8.266	330.

Table 3 Elastic and elastic plastic J-integral (kJ/m^2)
under pressure+ bending (a/c=1/4, a/c=1/3)

pressure(MPa)	moment kNm	Jel fond	Jpl fond	Jel surf	Jp surf
0	0.	0.	0.	0.	0.
5	0.	0.053	0.054	0.025	0.0245
10	0.	0.213	0.210	0.098	0.0999
14.2	0.	0.430	0.467	0.198	0.196
18.2	0.	0.707	1.05	0.326	0.42
21.2	0.	0.959	1.81	0.442	00698
21.2	5.15E+08	1.988	3.43	0.898	1.43
21.2	1.03E+09	3.379	7.48	1.512	3,29
21.2	1.41E+09	4.656	14.1	2.073	6.44
21.2	2.17E+09	7.798	51.2	3.45	24.8
21.2	2.94E+09	11.807	165.	5.202	84.
21.2	4.08E+09	19.295	682.	8.47	335.
21.2	5.23E+09	28.614	1490.	12.529	690.

Figure 0
Example of mesh (a/t = 1/4, a/c = 1/3)

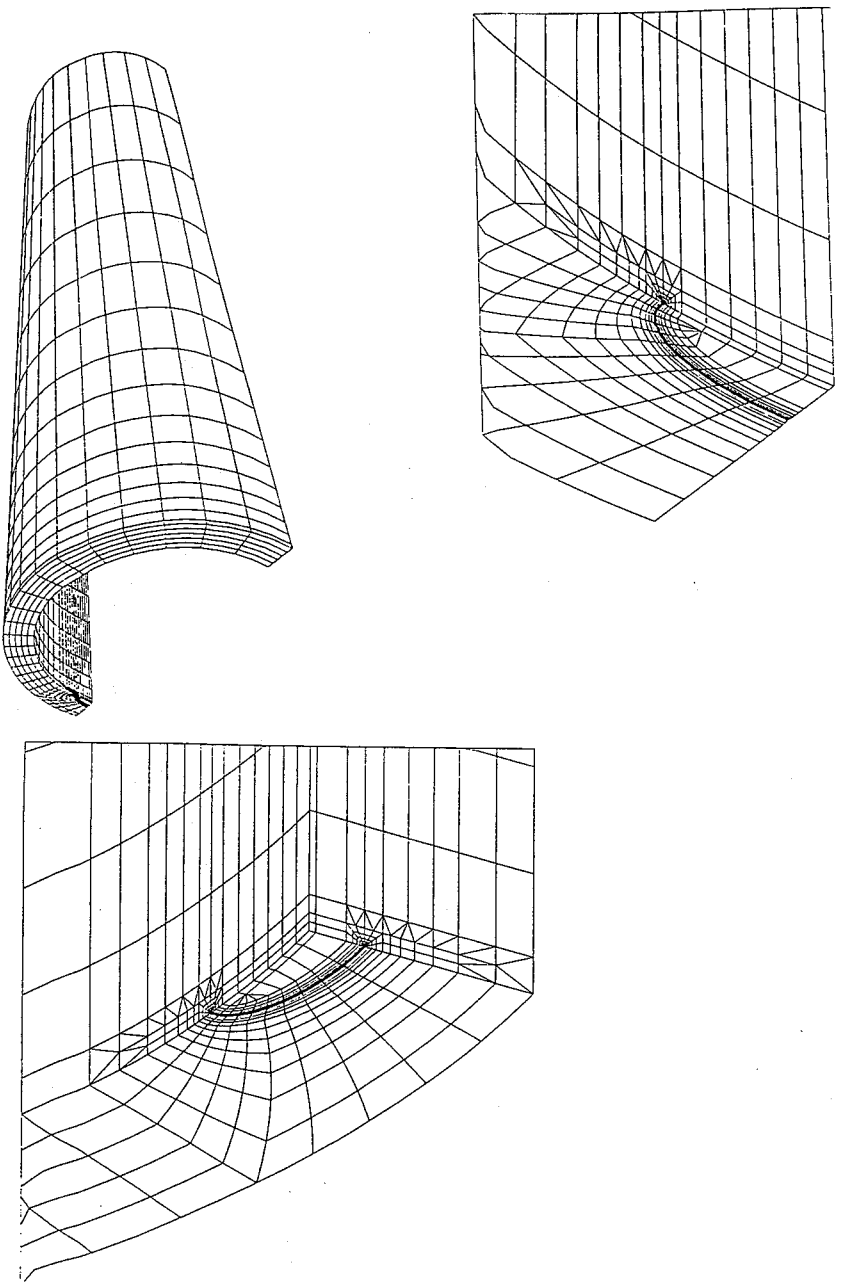

Figure 1 Comparison f.e. computation / RSE-M method
in bending a/t = 1/8 a/c = 1/3 deepest and surface point

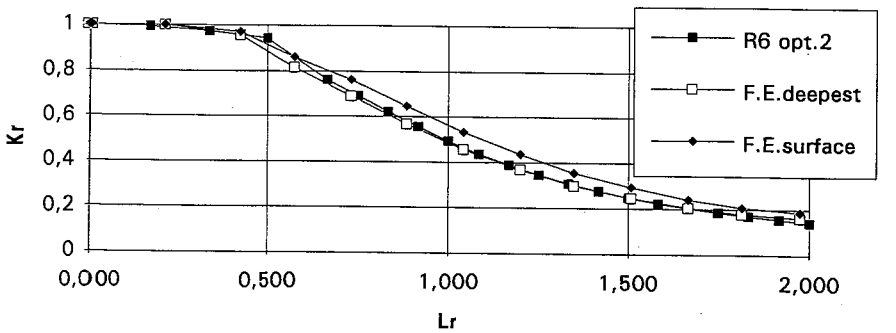

Figure 2 Comparison f.e.computation / RSE-M method
in bending a/t = 1/4 a/c = 1/10 deepest & surface point

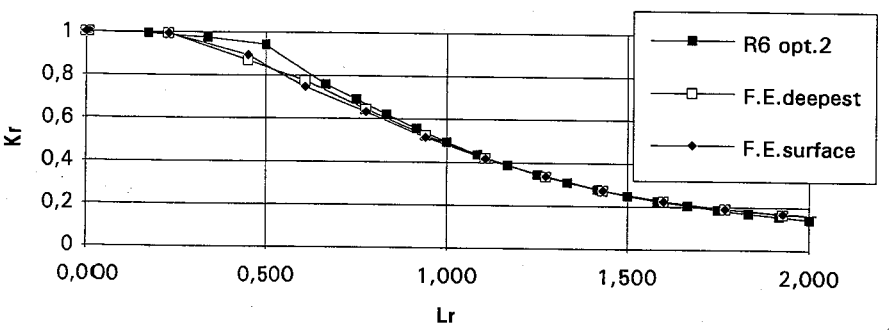

Figure 3 Comparison f.e.computation / RSE-M method
in bending a/t = 1/4 a/c = 1/3 deepest & surface point

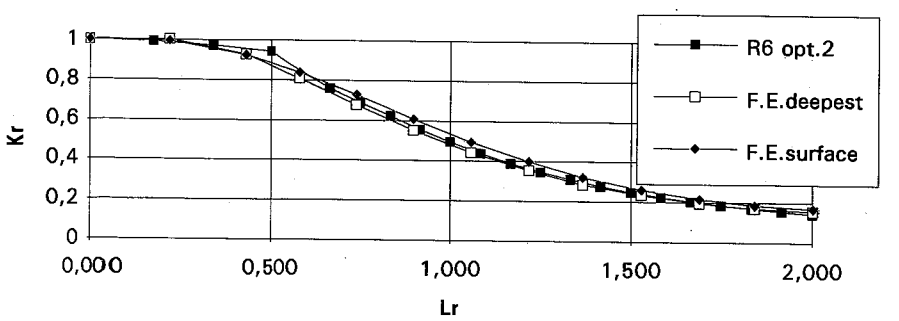

Figure 4 Comparison f.e.computation/RSE-M pressure+bending a/t=1/8 a/c=1/3 deepest & surface point

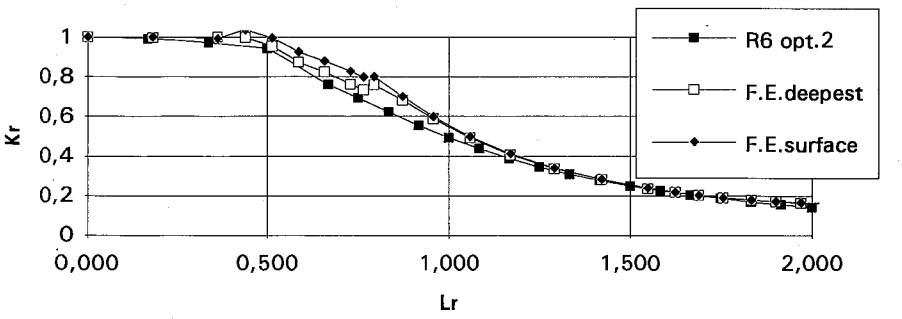

Figure 5 Comparison f.e.computation / RSE-M pressure+bending a/t=1/4 a/c=1/10 deep, surface pt

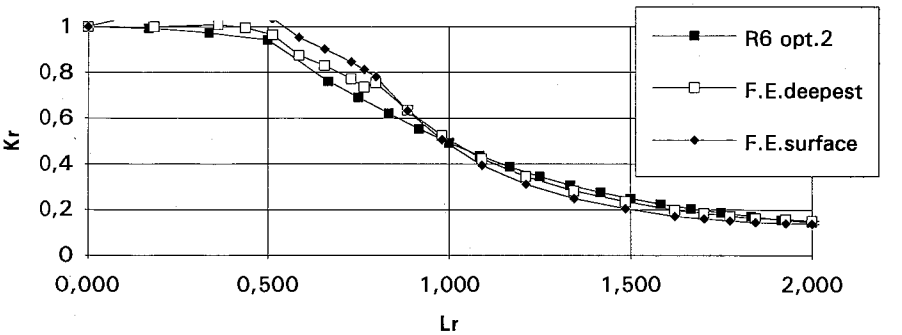

Figure 6 Comparison f.e.computation / RSE-M pressure+bending a/t=1/4 a/c=1/3 deep, surface pt